DOI: 10.1002/chem.200701472

# Engineering Nanorafts of Calixarene Polyphosphonates

**Thomas E. Clark,[a] Mohamed Makha,[a] Alexandre N. Sobolev,[a] Henry Rohrs,[b] Jerry L. Atwood,[c] and Colin L. Raston*[a]**

**Abstract:** The water-soluble calix[4]arene bearing *p*-substituted phosphonic acid groups is accessible in five steps in overall 62% yield, with the hydrogen-bonding prowess of the acidic groups dominating its self-assembly processes. These include the formation of 3.0(3) nm and 20(2) nm nanorafts of the calixarene in water using spinning disc processing, stabilized by acetonitrile, and nanorafts in the gas phase ($\leq$20 molecules). The 20(2) nm particles transform into 3.0(3) nm particles prior to crystallization into a compact bilayer, whereas crystallization in the presence of large organic molecules gives an expanded bilayer interposed by layers of water molecules.

**Keywords:** calixarenes · nanostructures · process intensification · self-assembly · supramolecular chemistry

## Introduction

Cavitand-type molecules contain a hydrophobic pocket, and whilst they can assemble into large nanometer-scale self-assembled architectures by noncovalent interactions, their ability to assembly into nanorafts is yet to be realized. This is despite a plethora of spectacular architectures having been established for cavitands, including nanocapsules, which are often based around the Platonic or Archimedean solids.[1–3] They can also describe complex entities found in nature such as certain types of protozoa, pollen grains, and crystals.[4]

Cavitand-type molecules include *C*-alkylresorcin[4]arenes and *C*-alkylpyrogallol[4]arenes, which can form hexameric capsules with an internal cavity of 1250–1375 Å$^3$.[5,6] The design characteristics of such cavitands is noteworthy in limiting intramolecular hydrogen bonding, leaving some hydroxy groups to participate in intermolecular hydrogen bonding, resulting in interplay of the cavitands, which can favor the formation of spheroid-like molecular capsules.

Calixarenes are another class of cavitands, which can be readily sulfonated, but generally it is the sulfonate group rather than the protonated sulfonic acid group that features in building complex arrays such as spheroid-like structures comprising twelve molecules at the vertices of icosahedra or cuboctahedra.[1,2] These water-soluble calixarenes are also of interest in relation to their ability to act as catalysts, surfactants, host molecules, and more.[7,8]

Herein we have targeted the corresponding calixarene with phosphonic acid groups in the *p*-position relative to the hydroxy groups at the base of the molecule, that is, *p*-phosphonic acid calix[4]arene, **1** (Scheme 1).

With two acidic hydrogen atoms now associated with each phosphonic acid functional group there is potential for forming complex arrays involving multiple hydrogen bonding associated with these groups, along with other inherently weak interactions such as π-stacking and C–H···π interplay. In contrast, there is only one acidic hydrogen atom for each functional group in the analogous sulfonated calixarene, and thus the calixarene has limited hydrogen-bonding capability. The lowest oligomer in the calixarene series has four phenol moieties, for which the calixarene is expected to take on the usually rigid bowl-shaped conformation associated with four intramolecular hydrogen bonds involving the phenolic hydroxy groups. Higher calixarenes are usually more flexible and may not necessarily adopt a cone- or bowl-shaped conformation.

[a] T. E. Clark, Dr. M. Makha, Dr. A. N. Sobolev, Prof. C. L. Raston
Department of Chemistry, The University of Western Australia
Crawley, WA 6009 (Australia)
Fax: (+61) 08-6488-1005
E-mail: clraston@chem.uwa.edu.au

[b] Dr. H. Rohrs
Department of Chemistry, University of Washington
St. Louis, MO 63130 (USA)

[c] Prof. J. L. Atwood
Department of Chemistry, University of Missouri-Columbia
Columbia, MO 65211 (USA)

Supporting information for this article is available on the WWW under http://www.chemeurj.org/ or from the author.

  

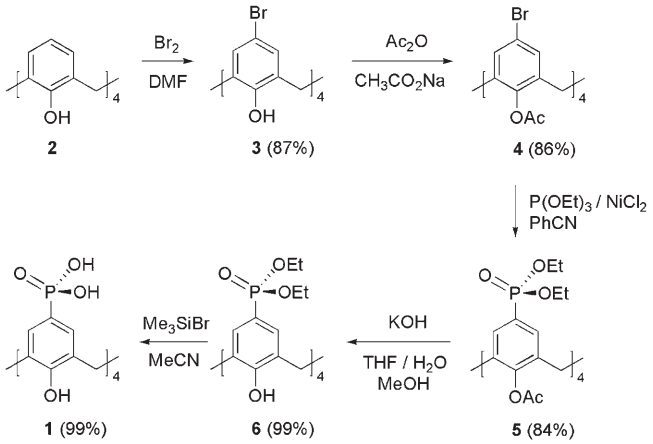


Scheme 1. Synthesis of *p*-phosphonic acid calix[4]arene. DMF = dimethylformamide, Ac = acetyl, Et = ethyl, Ph = phenyl, THF = tetrahydrofuran and Me = methyl.

The synthesis of compound **1** represented a synthetic challenge, in contrast to the ubiquitous one-step synthesis of the analogous sulfonic acid,[9] and we have established that **1** is accessible in five steps from the commercially available calix[4]arene in 62% overall yield (Scheme 1). Compound **1** indeed assembles into nanorafts using process intensification rotating surface (PIRS) technology, and into continuous structures based on bilayer arrangements, some of which are persistent in the gas phase. It is noteworthy that PIRS is a new method for fabricating nano-particles for which spinning disc processing (SDP) is rapidly developing;[10–12] the key components of SDP include a rotating disc with controllable speed, and feed jets located slightly off-center from the disc. SDP generates a thin fluid film (1–200 μm) on a rapidly rotating disc surface (300–3000 rpm), within which nano-arrays form (Figure 1),[12] with strong shearing forces creating turbulence and breaking the surface tension of the film, making waves and ripples.[11] These waves and ripples add to the vigor of mixing and ensure extremely short reaction residence time under plug flow conditions, with even mixing throughout the entire film. SDP is distinctly different from the well-known spin-coating process, which is the preferred method for the controlled coating of flat surfaces[13] ("discs") rather than being used for fabricating nanomaterials, as the application of SDP herein.

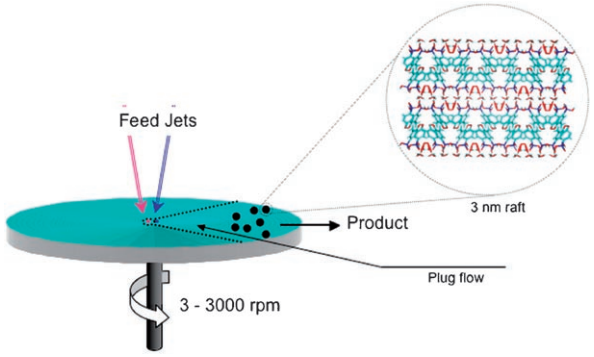


Figure 1. Key features of a spinning disc processor (SDP) used to fabricate 3.0(3) or 20(2) nm particles of compound **1** (inset shows the structure of a 3 nm particle).

## Results and Discussion

Multigram quantities of compound **1** were prepared by initially brominating calix[4]arene (**2**) using bromine to give the bromo-calixarene **3** in 87% yield (Scheme 1). Protection of the lower rim hydroxy groups by acetylation with acetic anhydride gave the tetra-acetate **4** in 86% yield, and subsequent phosphorylation with triethyl phosphite produced the corresponding phosphonate ester **5** in 84% yield. Deprotection of the acetyl groups was effected by using potassium hydroxide, which afforded **6** in quantitative yield. Thereafter, de-esterification of the ethoxy groups using bromotrimethylsilane (BTMS) gave **1**, also in quantitative yield.

Compound **1** is moderately soluble in dimethyl sulfoxide (DMSO), slightly soluble in cold water and alcohols such as methanol, and insoluble in all other common organic solvents. Slow evaporation of a saturated solution of **1** in methanol/6 N $HNO_3$/$Cu(NO_3)_2$ or water/curcumin afforded colorless single crystals suitable for X-ray diffraction studies, **1a** and **1b** respectively. Copper cations are not incorporated into structure **1a**, but their presence is necessary to effect crystallization. Changing the cation to rubidium, cesium, or nickel also gave colorless single crystals with the same unit cell dimensions, and thus these crystals are also devoid of metal ions. The overall structure, **1a**, is a compact bilayer arrangement with the bilayers linked together by hydrogen bonding between phosphonic acid groups from different bilayers. Crystallization from water in the presence of curcumin afforded structure **1b**. Changing curcumin to other organic molecules, such as β-carotene or carborane,[14] also yielded colorless crystals with the same unit cell dimensions. In the absence of such organic molecules we were unable to crystallize **1** from water. The structure of **1b** is very similar to that of **1a**, adopting the same bilayer arrangement, albeit now with the bilayers separated by a layer of water molecules (Figure 2 A and B).

Both structures crystallize in the same tetragonal space group *P4/n*, the major difference in cell dimensions being associated with the tetragonal *c* axis, 11.067(3) and 14.0678(8) Å for **1a** and **1b**, respectively. The tetragonal axis is normal to the bilayers with the cone-shaped calix[4]arenes residing on fourfold symmetry axes, and thus the difference in *c* axis is associated with the incorporation of a layer of water molecules for **1b** relative to **1a**. The *a* (and *b*) axes for the two structures are very similar (12.130(4) and 11.9381(6) Å for **1a** and **1b**, respectively), which reflects the similarity in packing within the bilayers in the two structures. In **1a** there is inclusion of a disordered methanol molecule in the cavity of the calixarenes with the methyl group directed towards the cavity. Similarly, in structure **1b** the cavity of each calixarene takes up a disordered water molecule. In both structures the calixarene adopts a crystallo-

  

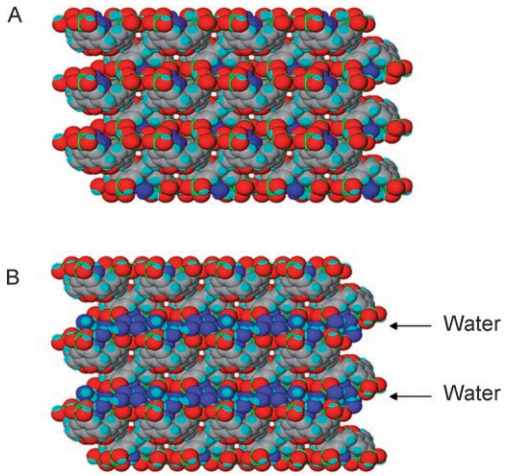


Figure 2. A) The compact bilayer organization of **1** in structure **1a**. B) The expanded bilayer organization of **1** in structure **1b**.

graphically imposed symmetrical cone conformation. This contrasts with a partially pinched cone conformation containing an ordered water molecule in the cavity of sulfonated calix[4]arene, which involves O–H···π interactions.[15] In both structures the phenolic hydroxy groups at the lower rim of the calixarene are engaged in a circular hydrogen-bonded network equally disordered in opposite directions (O–H···O distance is 1.82 and 1.83 Å for **1a** and **1b**, respectively).

The bilayer arrangements in both structures have calixarenes orientated in opposite directions, Figure 2 A and B. Both bilayers involve intricate hydrogen-bonding networks formed by bridging methanol or water molecules between phosphonic acid moieties within each bilayer (O–H···$OCH_3$ distances 1.78–2.05 Å for **1a**, and O–H···$OH_2$ distances 1.67–1.95 Å for **1b**) (Figure 3 A and B). In addition, methanol and water embedded in the cavity of both structures interacts with the inner walls of the calixarene via CH···π or OH···π interactions (short contacts for HOC···centroid and $H_2O$···centroid are 4.01 Å and 4.08 Å for **1a** and **1b**, respectively). The closest distance between phosphorus atoms of neighboring bilayers is 4.62 Å in **1a,** whereas it is 6.20 Å in **1b** where there is no hydrogen bonding between phosphonic acid groups across different bilayers. In **1a** the phosphonic acids are engaged in a complex hydrogen-bonding array forming a compact bilayer with a short contact –POH···O=$P(OH)_2$ of 1.61–1.75 Å, whereas in **1b** water molecules in the hydrophilic layer are interposed between bilayers with $OH_2$···O=$P(OH)_2$ and $H_2O$···HOPO(OH) distances ranging from 1.88–1.95 and 1.88–2.23 Å, respectively (Figure 3 A and B). A subtle difference in the packing of calixarenes within the bilayers is that in **1a** two methylene protons from a single carbon atom of one calixarene reside close to the face of an aromatic ring of another calixarene ($CH_2$···π interplay), whereas in **1b** only one of the hydrogen atoms from the same methylene group is associated with such an interaction.

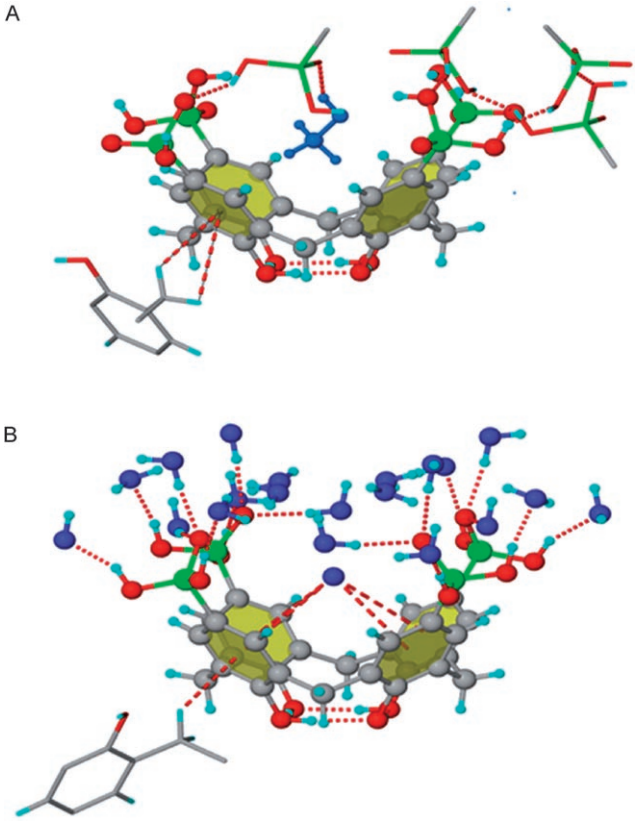


Figure 3. A) Building block for the assembly of **1a**; B) building block for the assembly of **1b**. (A and B) show the hydrogen bonding involved in the construction of the bilayers (ball-and-stick for one calixarene unit with neighboring calixarene fragments represented as sticks; water and methanol molecules depicted in blue and dashed and dotted lines represent hydrogen bonds).

Crystallization of compound **1** is also possible using SDP involving a 1 M sodium hydroxide solution containing **1** as the corresponding phosphonate and HCl solution at different concentrations (1.0, 1.5, 3.0, and 6.0 M). The experiment involved injecting the alkaline solution of **1** in one feed jet, and a solution of HCl in the other feed jet at room temperature (1 $mL\,s^{-1}$, grooved disc, 1500 rpm disc rotation) to ensure an acidic solution upon mixing. The spinning disc process induces rapid crystallization and is dependent on the molarity of the acid used, and generally yields micron-size particles. However, using HCl solutions containing 10% acetonitrile results in the formation of specifically 3.0(3) or 20(2) nm particles (dynamic light scattering) depending on the concentration of the acid (Figure 4 A and B); the ability to fabricate nanoparticles of a specific size, and stabilized by acetonitrile, under process intensification is noteworthy.

In the absence of acetonitrile, increasing the concentration of HCl induces immediate formation of micron-size particles which then re-disperse to form smaller particles upon standing for a few hours, notably 3.0(3) nm for 3 M HCl and 20(2) nm for 1.0 M HCl. The presence of acetonitrile circumvents the formation of micron size particles, affording stable 3.0(3) and 20(2) nm particles for 3.0 M and

  

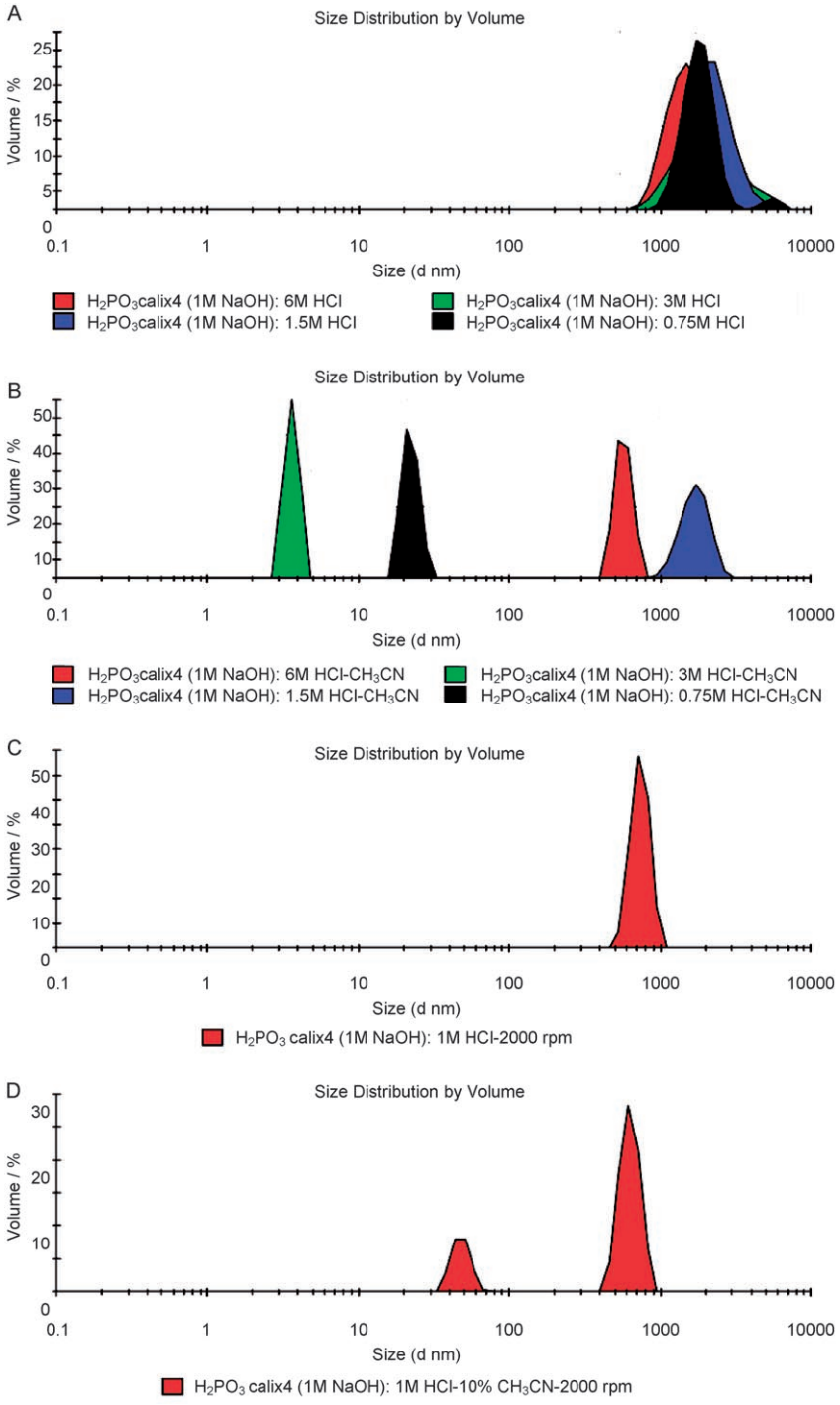


Figure 4. Volume size distributions of phosphonato-calix[4]arene nanoparticle dispersions. A and B) Various HCl concentrations at 1500 rpm using SDP without acetonitrile (A) and in the presence of 10% acetonitrile upon standing over an 18 hour period (B). C and D) 1 M HCl at 2000 rpm using SDP without acetonitrile (C) and in the presence of 10% acetonitrile upon standing over an 18-hour period (D).

1.0 M HCl, respectively (Figure 4A and B). Moreover, the particle size can also be controlled by varying the speed of the disc, amongst other parameters. For example, at 2000 rpm disc speed, 80(7) nm particles are formed for 1 M HCl, and the use of acetonitrile as a stabilizing agent in conjunction with SDP is critical (Figure 4C and D). Acetonitrile was selected for this purpose because of its ability to bind in the cavity of the calixarene on the surface of the nano-particles with the polar group directed to solution space in the same way as methanol does in **1a**.[16]

The X-ray powder diffraction (XRPD) pattern for the as-synthesized compound **1** (Scheme 1) matches the calculated powder pattern[17] for the aforementioned structure **1a** (Figure 5A–C).

Analysis of the peak widths using the Scherrer equation gave a particle size of 16–30 nm, which is comparable to that of the 20(2) nm particles formed by SDP. Precipitation of an aqueous solution of **1** with excess concentrated HCl produced a solid with the same crystal packing as the as-synthesized compound **1** (Figure 5D). Thus the packing of the calixarenes in the as-synthesized product is similar to the compact bilayer as seen for structure **1a**. Removal of the solvent for the above-prepared 3.0(3) nm particles (without acetonitrile) gave a diffraction pattern with a dominant peak at $2\theta = 9.0°$, which equates to a *d*-spacing of 1.0 nm, and matches closely the bilayer spacing in the compact bilayer of **1a** (Figure 5E).

The nanoraft assemblies also show remarkable stability in DMSO at room temperature, contrary to the fact that DMSO is effectively competing for hydrogen bond formation with the calixarene. Calixarene dimers have been shown to "denature" within seconds of addition of a small percentage of DMSO, which disrupts the hydrogen-bonded array holding the dimer together.[18] Thus our present system is intriguing, as the nanorafts slowly dissociate over the course of 36 h into solvated monomeric units (Figure 6).

A fresh deuterated DMSO solution of **1** gives a series of doublets for the two equivalent aromatic protons split by the single phosphorus environment in the $^1$H NMR spectrum. Over time the monomer doublet becomes dominant

  

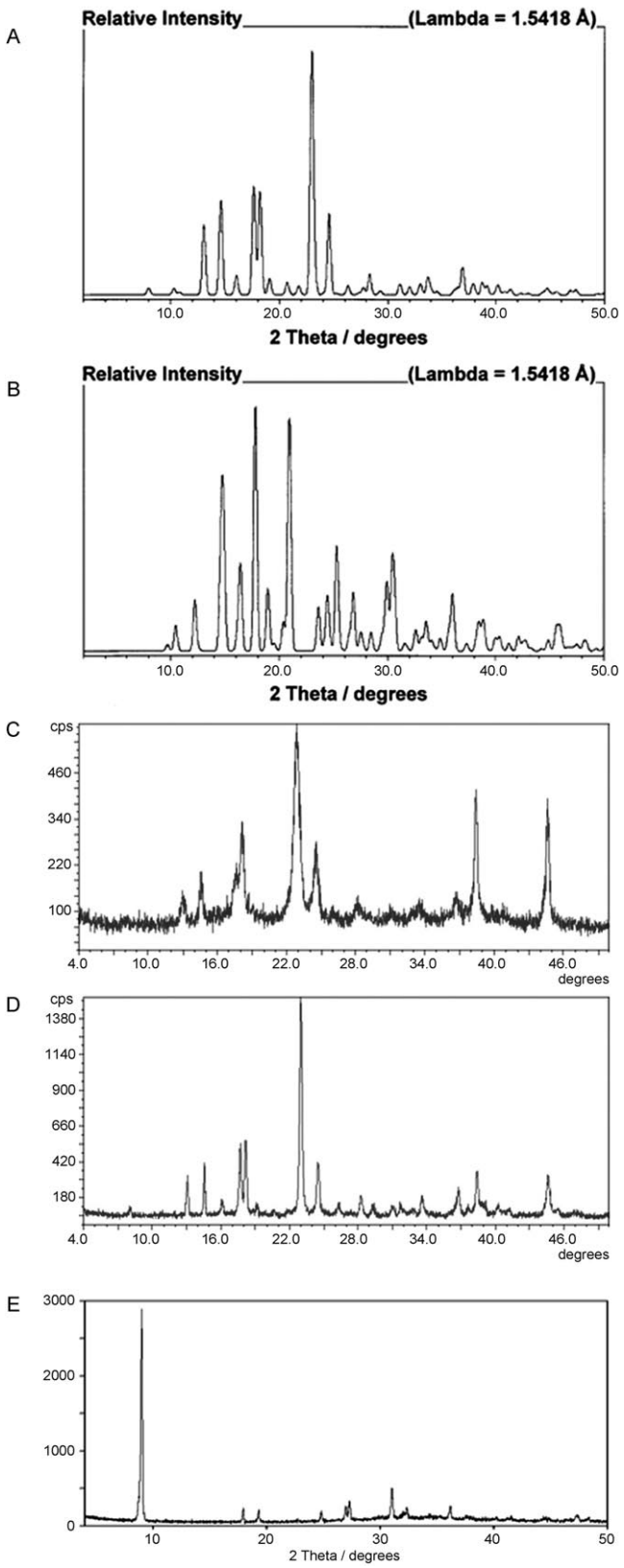


Figure 5. XRPD patterns of compound **1**. A) Calculated pattern for **1a**; B) calculated pattern for **1b**; C) experimental pattern for the as-synthesized solid; D) experimental pattern of the solid obtained by precipitation of an aqueous solution of **1** with concentrated HCl; E) experimental pattern of the product obtained by SDP using 1.0 M HCl. The peaks in (C) and (D) at 38.5 and 44.5° are background signals from the sample holder plate.

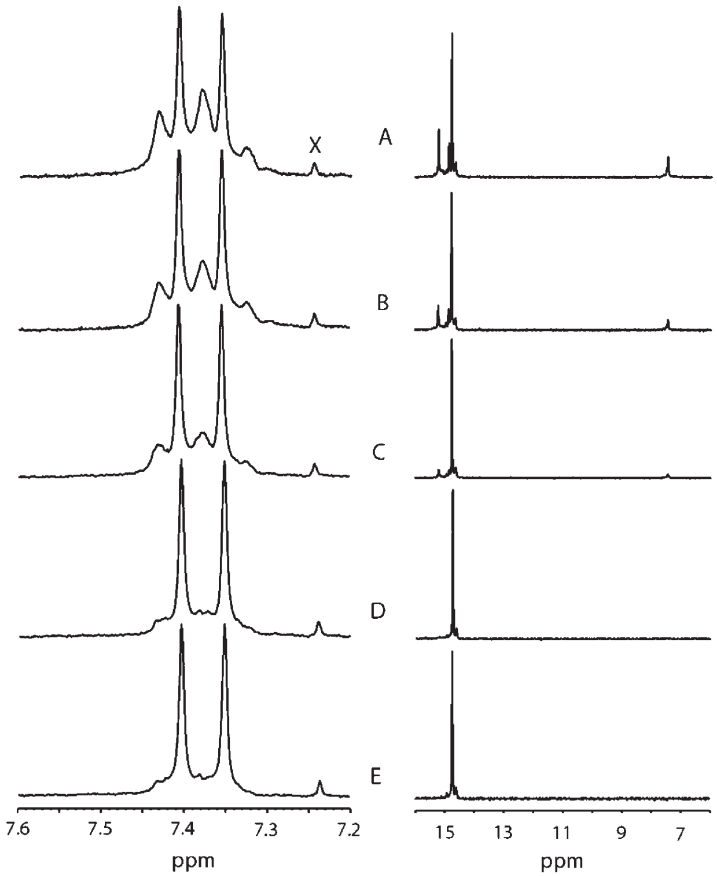


Figure 6. Expansion of the $^{1}$H NMR (left) and $^{31}$P NMR (right) of compound **1** between 7.6–7.2 and 16.0–6.0 ppm, respectively. A) 0 h; B) 3 h; C) 6 h; D) 18 h; E) 36 h. (X corresponds to an impurity).

as DMSO breaks up the nanorafts. This is confirmed by $^{31}$P NMR spectroscopy, which shows a series of multiplets around $\delta = 7$ and 14 ppm that converge to a singlet at $\delta =$ 14.7 ppm for the monomeric unit. The formation of nanorafts does not depend on the concentration or pH of the solution, but surprisingly its formation is sensitive to the presence of trace amounts of acetonitrile. One plausible explanation for this observation is that the residual acetonitrile in the as-synthesized solid is orchestrating the nanorafts' assembly. Acetonitrile has been shown to form a variety of hydrogen bonds with phenol in solution,[19] inclusion complexes with calixarenes,[16] and as surfactant stabilizers. Dynamic solution studies were attempted to establish the size of the nanorafts by using $^{31}$P NMR diffusion ordered spectroscopy (DOSY). However, due to the slow diffusing nature of the calixarene in DMSO the technique was not suitable. Compound **1** has solubility limitations except in protic solvents where nanorafts are not evident.

MALDI-TOF mass spectrometry on **1** provided further evidence for the compact bilayer packing in the solid state, showing fragmentation of the bilayer devoid of solvent (Figure 7 A).

The nanorafts were observed only when using an acidic matrix such as dihydroxybenzoic acid (DHB) and successive

  

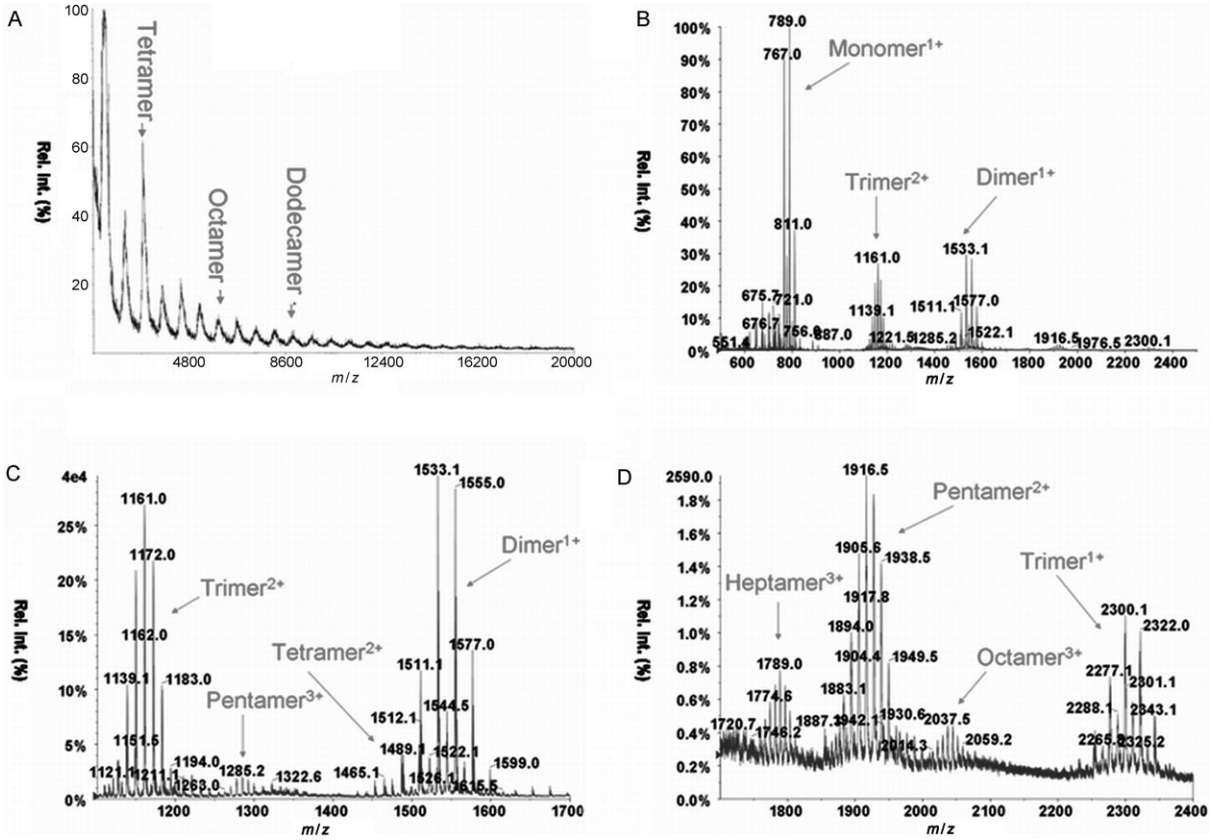


Figure 7. Mass spectra of compound **1**: A) MALDI-TOF spectrum showing nanoraft assemblies up to the 20-mer in the gas phase; B to D) ESI mass spectra between 500–2400 *m*/*z* (B), 1100–1700 *m*/*z* expansion (C), and 1700–2400 *m*/*z* expansion (D).

peaks out to the 20-mer were obtained. This is consistent with fragments of the continuous structure in complex **1a** being generated in the gas phase by the laser. These nanorafts can be viewed as fragments of the bilayers, with aggregates of four and six molecules of **1** showing particular stability. Attempts at detecting larger fragments, by increasing the extraction delay time and decreasing the laser power, were to no avail. These results are confirmed by ESI mass spectrometry in water or methanol, which show aggregates of up to eight molecules, also with no sign of associated solvent molecules (Figure 7 B–D). The nature of the structure of **1a** rules out any likelihood of the formation of spheroidal arrays of calixarenes, such as the Platonic and Archimedean solids, found in the *p*-sulfonato-calix[4]arene arrays of 12 calixarenes with all the cavities pointing away from the core of the arrays.[1,2] In addition there are no magic number signals in the mass spectrum corresponding to such structures. There is no evidence for the formation of nanoarrays of the water-containing complex **1b** in the gas phase.

## Conclusion

We have established the synthesis of a molecule that remarkably can be assembled into bilayers and nanorafts in a controlled way. The stability of the rafts in DMSO, especially in the presence of a critical concentration of acetonitrile, is testimony to the stability of the rafts, which are held together by a multitude of hydrogen bonds. A likely model for the structure of the rafts is that established in the continuous structure for the compound crystallized from an acidic solution of methanol in the presence of metal ions.

The ability to self-assemble molecules into nanoarrays using PIRS technology is, in itself, a new paradigm in self-assembly, and the findings have implications for the engineering of nanoparticles of a wide range of organic molecules. The findings show that the lowest oligomer of the *p*-phosphonic acid calixarenes has a remarkable ability to self-assemble into bilayers, with the ability to engineer material with water between bilayers or engineer bilayers devoid of such water molecules, and possibly the ability to engineer particles of particular shapes as well as size. The scene is now set to translate this to the higher phosphonated calixarenes.

## Experimental Section

**General**: All starting materials and solvents were obtained from commercial suppliers and used without further purification unless otherwise noted. Acetonitrile was dried over 4 Å molecular sieves for 24 h, and $NiCl_2 \cdot 6H_2O$ was dried at 180 °C in vacuo for 8 h before use. All mois-

  

ture-sensitive reactions were performed under a positive pressure of nitrogen. Calix[4]arene was prepared as described previously in the literature.[20] Bromo-calixarene **3** and the tetra-acetate **4** were prepared by a modified literature procedure for the corresponding calix[8]arenes.[21] The phosphonate ester **5** was prepared by a nickel-catalyzed Arbuzov reaction,[22] and complete deacetylation and de-esterification to give **1** was accomplished using well-known procedures.[23] All MALDI mass spectra were recorded by using a Perseptive Voyager DE-RP and all ESI spectra were recorded on a Thermo Scientific LTQ-FT. A full description of the methods used can be found in the Supporting Information.

CCDC-649194, CCDC-649195, CCDC-649196, CCDC-649197, CCDC-649198, CCDC-649199 contain the supplementary crystallographic data for this paper. These data can be obtained free of charge from The Cambridge Crystallographic Data Centre via www.ccdc.cam.ac.uk/data_request/cif.

**5,11,17,23-Tetrabromo-25,26,27,28-tetrahydroxycalix[4]arene (3)**: Bromine (7.25 mL, 0.14 mol) in DMF (100 mL) was added dropwise with stirring to a solution of calix[4]arene (10.00 g, 23.58 mmol) in DMF (400 mL). The solution was stirred for 4 h with a precipitate forming after about 0.5 h. Methanol (400 mL) was added and the mixture left to stir for 0.5 h. The precipitate was filtered off and washed with methanol (3×50 mL) to yield **3** (15.16 g, 87%) as a white solid. $^1$H NMR ([D$_6$]DMSO, 25°C, 300 MHz): $\delta$=7.35 (s, 8H, ArH), 3.82 ppm (br s, 8H, ArC*H*$_2$Ar).

**5,11,17,23-Tetrabromo-25,26,27,28-tetraacetoxycalix[4]arene (4)**: A mixture of **3** (7.32 g, 9.94 mmol) and anhydrous sodium acetate (4.89 g, 59.65 mmol) in acetic anhydride (120 mL) was refluxed for 4 h. After cooling to room temperature, the solution was slowly quenched with water (150 mL). The precipitate was filtered off and washed with methanol (3×30 mL) to yield **4** (7.72 g, 86%) as a white solid. Recrystallization from chloroform yielded X-ray quality single crystals, **4a** and **4b**, which were also submitted for microanalysis. m.p. >290°C (decomp); IR (KBr): $\tilde{\nu}$=2919 (w), 1753 (s), 1571 (w), 1458 (m), 1368 (m), 1211 (s), 1179 (s), 873 (m) cm$^{-1}$; $^1$H NMR ($CDCl_3$, 25°C, 600 MHz): $\delta$=7.22 (s, 8H, ArH), 3.65 (s, 8H, ArC*H*$_2$Ar), 1.74 ppm (s, 12H, CH$_3$); $^{13}$C NMR ($CDCl_3$, 25°C, 151 MHz): $\delta$=167.43, 147.24, 134.82, 132.20, 118.67, 37.04, 20.22 ppm; HRMS (FAB): *m/z* calcd for [C$_{36}$H$_{28}$Br$_4$O$_8$ + H]$^+$ 908.8555, found 908.8518; elemental analysis calcd (%) for C$_{36}$H$_{28}$Br$_4$O$_8$: C 47.61, H 3.11; found: C 47.98, H 3.36. Crystal/refinement details for **4a**: C$_{39}$H$_{31}$Br$_4$Cl$_9$O$_8$, $M_r$=1266.33, $F$(000)=1244 e, triclinic, $P\bar{1}$ (no. 2), $Z$=2, $T$=153(2) K, $a$=13.171(2), $b$=13.487(2), $c$=15.014(2) Å, $\alpha$=95.498(2), $\beta$=93.609(2), $\gamma$=114.844(2)°, $V$=2393.3(6) Å$^3$, $\rho_{calcd}$=1.757 g cm$^{-3}$, sin$\theta/\lambda_{max}$=0.5953, $N$(unique)=8258, (merged from 16787, $R_{int}$=0.0461, $R_{sig}$=0.0634), $N_o$ ($I>2\sigma(I)$)=6811, $R$=0.0369, *wR2*=0.0978 ($A$,$B$=0.04, 0.00), GOF=1.093, $|\Delta\rho_{max}|$=1.1(1) e Å$^{-3}$. Crystal/refinement details for **4b**: C$_{73}$H$_{57}$Br$_8$Cl$_3$O$_{16}$, $M_r$=1935.82, $F$(000)=7632 *e*, orthorhombic, *Ccca* (no. 68), $Z$=8, $T$=100(2) K, $a$=18.5752(2), $b$=35.9383(3), $c$=22.7037(2) Å, $V$=15156.1(2) Å$^3$, $\rho_{calcd}$=1.697 g cm$^{-3}$, $\mu_{Cu}$=6.576 mm$^{-1}$, sin$\theta/\lambda_{max}$=0.5878, $N$(unique)=6458 (merged from 85783, $R_{int}$=0.0475, $R_{sig}$=0.0158), $N_o$ ($I>2\sigma(I)$)=6042, $R$=0.0872, *wR2*=0.2250 ($A$,$B$=0.055, 800.0), GOF=1.033, $|\Delta\rho_{max}|$=1.1(1) e Å$^{-3}$.

**5,11,17,23-Tetra(diethoxyphosphoryl)-25,26,27,28-tetraacetoxycalix[4]arene (5)**: A solution of **4** (5.51 g, 6.10 mmol) and $NiCl_2$ (0.79 g, 6.10 mmol) in benzonitrile (10 mL) was treated dropwise with P(OEt)$_3$ (10.45 mL, 60.96 mmol) under nitrogen at 190°C. The solution was stirred for 0.5 h and the volatiles were removed under reduced pressure to leave an orange residue. The residue was purified by flash chromatography to yield **5** (5.83 g, 84%) as a light yellow solid. Recrystallization from toluene or ethyl acetate yielded X-ray quality single crystals **5a** and **5b**, respectively, which were also submitted for microanalysis. R$_f$ 0.44 (1:4 methanol–ethyl acetate); m.p. 251–253°C; IR (KBr): $\tilde{\nu}$=2985 (m), 2911 (m), 1755 (s), 1650 (w), 1464 (m), 1374 (m), 1267 (m), 1020 (s), 970 (s), 796 (w), 609 (m) cm$^{-1}$; $^1$H NMR ($CDCl_3$, 25°C, 500 MHz): $\delta$=7.52 (d, 8H, $J_{P\text{-}H}$=13.0 Hz; ArH), 4.20–4.05 (m, 16H, POCH$_2$), 3.79 (s, 8H, ArC*H*$_2$Ar), 1.67 (s, 12H, CH$_3$), 1.31 ppm (t, 24H, $J$=7.0 Hz, POCH$_2$C*H*$_3$); $^{13}$C NMR ($CDCl_3$, 25°C, 126 MHz): $\delta$=167.31, 151.22 (d, $^4J_{P\text{-}C}$=4.2 Hz), 133.27 (d, $^3J_{P\text{-}C}$=16.2 Hz), 132.72 (d, $^2J_{P\text{-}C}$=10.4 Hz), 126.15 (d, $^1J_{P\text{-}C}$=192.5 Hz), 62.22 (d, $^2J_{P\text{-}C}$=6.0 Hz), 37.24, 20.07, 16.35 ppm (d, $^3J_{P\text{-}C}$=6.4 Hz); $^{31}$P NMR ($CDCl_3$, 25°C, 202 MHz): $\delta$=17.79 ppm; HRMS (FAB) *m/z* calcd for [C$_{52}$H$_{68}$O$_{20}$P$_4$ + H]$^+$ 1137.3333, found 1137.3363; elemental analysis calcd (%) for C$_{52}$H$_{68}$O$_{20}$P$_4$ + 1.2 H$_2$O: C 53.91, H 6.12; found: C 53.66, H 5.86. Crystal/refinement details for **5a**: C$_{55.50}$H$_{74}$O$_{21}$P$_4$, $M_r$=1201.03, $F$(000)=2540 e, triclinic, $P\bar{1}$ (no. 2), $Z$=4, $T$=153(2) K, $a$=13.410(2), $b$=17.619(2), $c$=27.760(4) Å, $\alpha$=103.086(2), $\beta$=91.709(2), $\gamma$=108.046(2)°, $V$=6038.8(14) Å$^3$, $\rho_{calcd}$=1.321 g cm$^{-3}$, sin$\theta/\lambda_{max}$=0.5946, $N$(unique)=21084 (merged from 46491, $R_{int}$=0.0386, $R_{sig}$=0.0631), $N_o$ ($I>2\sigma(I)$)=14021, $R$=0.0689, *wR2*=0.1790 ($A$,$B$=0.10, 8.52), GOF=1.042, $|\Delta\rho_{max}|$=1.4(1) e Å$^{-3}$. Crystal/refinement details for **5b**: C$_{108}$H$_{148}$O$_{44}$P$_8$, $M_r$=2398.02, $F$(000)=2536 e, triclinic, $P\bar{1}$ (no. 2), $Z$=2, $T$=153(2) K, $a$=13.547(2), $b$=17.641(3), $c$=27.463(5) Å, $\alpha$=102.591(2), $\beta$=92.803(2), $\gamma$=109.046(2)°, $V$=6003.2(17) Å$^3$, $\rho_{calcd}$=1.327 g cm$^{-3}$, sin$\theta/\lambda_{max}$=0.5964, $N$(unique)=20010 (merged from 37575, $R_{int}$=0.0361, $R_{sig}$=0.0630), $N_o$ ($I>2\sigma(I)$)=13894, $R$=0.1028, *wR2*=0.2774 ($A$,$B$=0.17,17.15), GOF=1.064, $|\Delta\rho_{max}|$=1.7(1) e Å$^{-3}$.

**5,11,17,23-Tetra(diethoxyphosphoryl)-25,26,27,28-tetrahydroxycalix[4]arene (6)**: A mixture of **5** (2.50 g, 2.20 mmol) and KOH (1.23 g, 22.00 mmol) in methanol (50 mL), tetrahydrofuran (50 mL) and water (50 mL) was stirred for 4 h. The solvents were removed under reduced pressure and the residue treated with dichloromethane (50 mL) and 2N HCl (50 mL). The organic layer was separated, washed with 2N HCl (1×25 mL), water (2×25 mL), dried over $MgSO_4$ and evaporated under reduced pressure to yield **6** (2.10 g, 99%) as a light yellow solid. Recrystallization from ethyl acetate/hexane yielded a white solid suitable for microanalysis. m.p. 126–128°C; IR (KBr): $\delta$=3307 (br), 2984 (m), 2906 (m), 1599 (m), 1478 (m), 1392 (w), 1284 (m), 1022 (s), 963 (s), 790 (m) cm$^{-1}$; $^1$H NMR ($CDCl_3$, 25°C, 600 MHz): $\delta$=10.27 (br s, 4H, OH), 7.56 (d, 8H, ArH, $J_{P\text{-}H}$=13.2 Hz), 4.26 (br s, 4H, ArC*H*HAr), 4.11–4.02 (m, 8H, POC*H*HCH$_3$), 4.02–3.94 (m, 8H, POCH*H*CH$_3$), 3.69 (br s, 4H, ArCH*H*Ar), 1.27 ppm (t, 24H, POCH$_2$C*H*$_3$, $J$=7.2 Hz); $^{13}$C NMR ($CDCl_3$, 25°C, 151 MHz): $\delta$=152.30 (d, $^4J_{P\text{-}C}$=3.6 Hz), 133.38 (d, $^2J_{P\text{-}C}$=10.7 Hz), 127.72 (d, $^3J_{P\text{-}C}$=16.3 Hz), 122.25 (d, $^1J_{P\text{-}C}$=193.9 Hz), 62.09 (d, $^2J_{P\text{-}C}$=5.6 Hz), 31.42, 16.28 ppm (d, $^3J_{P\text{-}C}$=6.3 Hz); $^{31}$P NMR ($CDCl_3$, 25°C, 202 MHz): $\delta$=18.73; HRMS (FAB): *m/z* calcd for [C$_{44}$H$_{60}$O$_{16}$P$_4$ + 2H]$^+$ 970.2988, found 970.2940; elemental analysis calcd (%) for C$_{44}$H$_{60}$O$_{16}$P$_4$ + 0.35 H$_2$O: C 54.20, H 6.27; found: C 53.93, H 5.96.

**5,11,17,23-Tetra(dihydroxyphosphoryl)-25,26,27,28-tetrahydroxycalix[4]arene (1)**: Bromotrimethylsilane (4.75 mL, 36.02 mmol) was added to **6** (2.18 g, 2.25 mmol) in dry acetonitrile (50 mL) and the solution was refluxed for 16 h. The volatiles were removed under reduced pressure and the resulting residue was triturated with acetonitrile (40 mL) and water (2 mL). The precipitate formed was filtered off and washed with acetonitrile (3×20 mL) to yield **1** (1.65 g, 99%) as a white solid. Recrystallization from methanol/6N $HNO_3$/Cu(NO$_3$)$_2$ or water/curcumin yielded X-ray quality single crystals **1a** and **1b**, respectively, which were also submitted for microanalysis. m.p. 233–235°C (decomp); IR (KBr): $\tilde{\nu}$=3174 (br), 2300 (br), 1600 (m), 1473 (m), 1384 (m), 1275 (m), 1133 (s), 983 (s), 885 (m) cm$^{-1}$; $^1$H NMR ([D$_6$]DMSO, 25°C, 500 MHz): $\delta$=7.39 (d, 8H, Ar*H*, $J_{P\text{-}H}$=13.0 Hz), 5.73 (br s, CO*H*/PO*H*, shifts downfield with increasing [H]$^+$), 3.93 ppm (br s, 8H, ArC*H*$_2$Ar); $^{13}$C NMR ([D$_6$]DMSO, 25°C, 126 MHz): $\delta$=154.03, 131.67 (d, $^2J_{P\text{-}C}$=10.1 Hz), 127.74 (d, $^3J_{P\text{-}C}$=15.1 Hz), 124.65 (d, $^1J_{P\text{-}C}$=186.1 Hz), 31.09 ppm; $^{31}$P NMR ([D$_6$]DMSO, 25°C, 101 MHz): $\delta$=14.74; MS (ESI) *m/z* calcd for [C$_{28}$H$_{28}$O$_{16}$P$_4$ + H]$^+$ 745.04, found 745.04; elemental analysis calcd (%) for C$_{28}$H$_{28}$O$_{16}$P$_4$ + 0.5 H$_2$O + CH$_3$OH: C 44.35, H 4.23; found: C 44.04, H 4.61. Crystal/refinement details for **1a**: C$_{29}$H$_{33}$O$_{17.5}$P$_4$, $M$=785.43, $F$(000)=814 *e*, tetragonal, *P4/n*, $Z$=2, $T$=173(2) K, $a$=12.130(4), $c$=11.067(3) Å, $V$=1628.4(7) Å$^3$, $\rho_{calcd}$=1.602 g cm$^{-3}$, sin$\theta/\lambda_{max}$=0.5552, $N$(unique)=1161 (merged from 4657, $R_{int}$=0.0615, $R_{sig}$=0.0597), $N_o$ ($I>2\sigma(I)$)=801, $R$=0.0960, *wR2*=0.2116 ($A$,$B$=0.09, 18.00), GOF=1.002, $|\Delta\rho_{max}|$=1.0(1) e Å$^{-3}$. Crystal/refinement details for **1b**: C$_{28}$H$_{48}$O$_{26}$P$_4$, $M_r$=924.54, $F$(000)=968 *e*, tetragonal, *P4/n*, $Z$=2, $T$=100(2) K, $a$=11.9381(6), $c$=14.0678(8) Å, $V$=2004.92(15) Å$^3$, $\rho_{calcd}$=1.531 g cm$^{-3}$, sin$\theta/\lambda_{max}$=0.5946, $N$(unique)=1758 (merged from 15584, $R_{int}$=0.0891, $R_{sig}$=0.0721), $N_o$ ($I>2\sigma(I)$)=1492, $R$=0.1238, *wR2*=0.2503 ($A$,$B$=0.10, 13.40), GOF=1.185, $|\Delta\rho_{max}|$=0.8(1) e Å$^{-3}$.

  

## Acknowledgements

We thank the ARC, NSF and NIH (grant P41RR00954) for financial support of this work and The University of Western Australia for SIRF, GRST and PRT awards to Thomas Clark.

[1] G. W. Orr, L. J. Barbour, J. L. Atwood, *Science* **1999**, *285*, 1049–1052.
[2] J. L. Atwood, L. J. Barbour, S. J. Dalgarno, M. J. Hardie, C. L. Raston, H. R. Webb, *J. Am. Chem. Soc.* **2004**, *126*, 13170–13171.
[3] K. Kobayashi, T. Shirasaka, K. Yamaguchi, S. Sakamoto, E. Horn, N. Furukawa, *Chem. Commun.* **2000**, 41–42.
[4] S. Alvarez, *Dalton Trans.* **2005**, 2209–2233.
[5] L. R. MacGillivray, J. L. Atwood, *Nature* **1997**, *389*, 469–472.
[6] S. J. Dalgarno, S. A. Tucker, D. B. Bassil, J. L. Atwood, *Science* **2005**, *309*, 2037–2039.
[7] S. Shinkai, S. Mori, H. Koreishi, T. Tsubaki, O. Manabe, *J. Am. Chem. Soc.* **1986**, *108*, 2409–2416.
[8] S. J. Dalgarno, J. L. Atwood, C. L. Raston, *Chem. Commun.* **2006**, 4567–4574.
[9] S. Shinkai, *Pure Appl. Chem.* **1986**, *58*, 1523–1528.
[10] L. M. Cafiero, G. Baffi, A. Chianese, R. J. J. Jachuck, *Ind. Eng. Chem. Res.* **2002**, *41*, 5240–5246.
[11] R. J. J. Jachuck, C. Ramshaw, *Heat Recovery Syst. CHP* **1994**, *14*, 475–491.
[12] N. Anantachoke, M. Makha, C. L. Raston, V. Reutrakul, N. C. Smith, M. Saunders, *J. Am. Chem. Soc.* **2006**, *128*, 13847–13853.
[13] W. W. Flack, D. S. Soong, A. T. Bell, D. W. Hess, *J. Appl. Phys.* **1983**, *56*, 1199–1206.
[14] For references on carborane-facilitated crystallization without incorporation of carborane see: T. E. Clark, M. Makha, C. L. Raston, A. N. Sobolev, *CrystEngComm* **2006**, *8*, 707–711.
[15] J. L. Atwood, F. Hamada, K. D. Robinson, G. W. Orr, R. L. Vincent, *Nature* **1991**, *349*, 683–684.
[16] M. J. Hardie, C. L. Raston, S. Salinas, *Chem. Commun.* **2001**, 1850–1851.
[17] XRPD patterns were calculated using the program Lazy Pulverix.
[18] R. K. Castellano, S. L. Craig, C. Nuckolls, J. Rebek, Jr., *J. Am. Chem. Soc.* **2000**, *122*, 7876–7882.
[19] E. S. Kryachko, M. T. Nguyen, *J. Phys. Chem. A* **2002**, *106*, 4267–4271.
[20] *Macrocycle Synthesis: A Practical Approach* (Ed.: D. Parker), Oxford University Press, Oxford, **1996**.
[21] V. Böhmer, V. Brusko, K. Rissanen, *Synthesis* **2002**, *13*, 1898–1902.
[22] V. I. Kalchenko, L. I. Atamas′, V. V. Pirozhenko, L. N. Markovskii, *Zh. Obshch. Khim.* **1992**, *62*, 2623–2625.
[23] H. L. Hgo, W. Lin, *J. Am. Chem. Soc.* **2002**, *124*, 14298–14299.

Received: September 17, 2007
Published online: March 11, 2008

  